Optimization of Segmented Blank Holder Shape and Its Variable Blank Holder Gap in Deep-Drawing Process

Journal of Advanced Mechanical Design, Systems, and Manufacturing

Vol. 6, No. 4, 2012

Optimization of Segmented Blank Holder Shape and Its Variable Blank Holder Gap in Deep-Drawing Process*

Jirasak SRIRAT**, Koetsu YAMAZAKI*** and Satoshi KITAYAMA***

**Graduate School of Natural Science and Technology, Kanazawa University, Kakuma-machi, Kanazawa, 920-1192 Japan

E-mail: jirasak@stu.kanazawa-u.ac.jp

***Kanazawa University, Kakuma-machi, Kanazawa, 920-1192, Japan

Abstract

Optimum segmented blank holder shape and its variable blank holder gaps (VBHGs) are determined by a sequential approximate optimization (SAO) with radial basis function network. In deep drawing, wrinkling and tearing of blank sheet are major defects. The optimum segmented blank holder shape and its VBHGs are determined to avoid these defects. The Forming Limit Diagram (FLD) is employed to evaluate quantitatively the wrinkling and the tearing. In the numerical examples, a square cup deep drawing is handled. The objective is to minimize the thickness deviation after sheet forming. The wrinkling and the tearing are separately evaluated as the constraints. The dimensions of the segmented blank holder shape and the BHGs are taken as the design variables. The optimization result shows that simultaneous optimization of both the segmented blank holder shape and the VBHGs is one of the effective approaches for improving product quality.

Key words: Deep Drawing, Computer Aided Engineering, Engineering Optimization, Blank Holder Gap, Segmented Blank Holder Shape

1. Introduction

In sheet forming, wrinkling and tearing are major defects. In order to avoid these defects before manufacturing, numerical simulation based on finite element analysis (FEA) is a powerful tool [(1)]. To avoid these defects, many parameters, such as tools geometry, blank material properties, lubrication, blank holder force (BHF), blank holder gap (BHG), and so on, should be appropriately adjusted. Among them, one of the most effective parameters is to control blank holder force (BHF) and blank holder gap (BHG).

Many papers proposed the algorithms to control the BHF during forming process, that are often called variable blank holder force (VBHF) [(2-6)]. The BHF is applied to the blank holder for clamping the blank sheet between blank holder and die. In order to suppress wrinkling, the BHF will be increased. In numerical simulations, flange wrinkling height (FWH) illustrated in Fig. 1 is widely used for the wrinkling detection [(6)]. Therefore, the

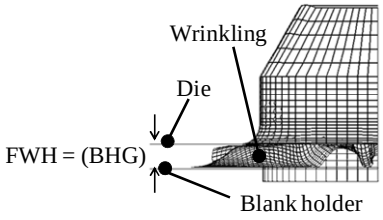

Fig. 1 Wrinkling in numerical simulation [(6)]

*Received 5 Jan., 2012 (No. 12-0005)
[DOI: 10.1299/jamdsm.6.420]

wrinkling can be observed when the distance between blank holder and die is larger than a critical value. It is clear from Fig. 1 that the FWH is equal to the BHG. In contrast, maximum thinning is generally used for tearing.

The VBHF is one of the effective approaches for avoiding defects. In the VBHF approach, the BHF will vary through the punch stroke. Thus, the objective of the VBHF approach is to find the VBHF trajectory through the punch stroke. The VBHF approaches can be roughly classified into two categories: One is based on the closed-loop type algorithm and the other is the response surface method (RSM) [7-12]. The authors have already proposed both approaches for avoiding these defects, and the detailed procedures can be found in Refs. (6) and (12). The VBHF can be indirectly controlled by the gap between the blank holder and the die. As the result, a large time delay of VBHF control can be observed in the experiment [6]. Then, the BHG approach may be employed to reduce the delay of the controlling that leads to the improvement of product quality. Osakada et al. [13] suggested that the BHG and the BHF should be simultaneously controlled in deep drawing process. It is expected that more direct control of the gap between the blank holder and the die can be achieved with the BHG control, in comparison with the VBHF approach. In addition, when the BHG approach is employed, the BHF is small at the beginning of punch stroke that is good for material flow into a die [14]. Therefore, we focus on the BHG approach for avoiding wrinkling and tearing in this paper.

Wang et al. [14] recommended determining an appropriate BHG for deep drawing process, which an appropriate BHG was determined by trial-and-error method. Chen et al. [15] examined the effect of BHG on deep drawing process. They reported that the BHG has a great effect on the product. Gavas et al. [16] examined the effect of BHG through experiments, and found an appropriate BHG to avoid the defects. In research on the BHG approach, an appropriate BHG was determined by trial-and-error method. In addition, a constant BHG is employed through the punch stroke. The constant BHG cannot control effectively the material flow. In order to control effectively the material flow, a variable BHG (VBHG) trajectory that the BHG will vary through punch stroke should be adopted.

In addition, we consider the segmented blank holder shape. Here, let us explain about the segmented blank holder shape by using Fig. 2. Figure 2 shows a quarter model of square cup deep drawing that the blank holder shape is divided into three segments. Considering the symmetry, the segmented blank holder shape consists of two parts: the straight part, and the corner part. This segmented blank holder shapes can be expressed by three design variables; length (L), width (D) and divided angle (A) as shown in Fig. 2. These design variables may affect the product, but these are determined by experiences.

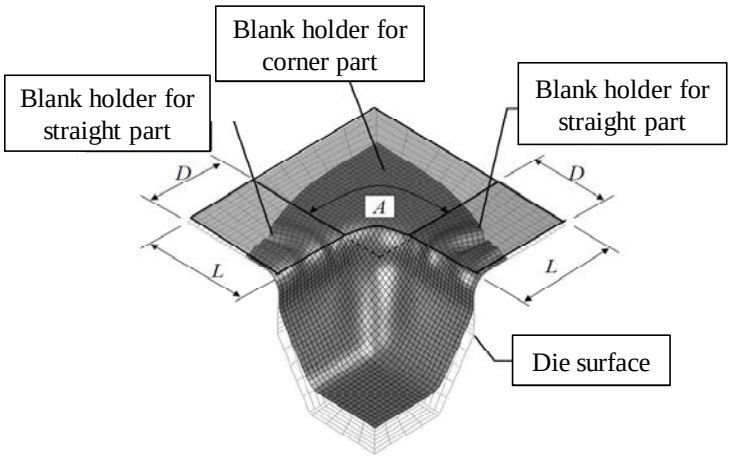

Fig. 2 Design variables to determine the segmented blank holder shape

In sheet forming simulations, much computational cost is generally required. Under such situations, the RSM is one of the practical approaches. A sequential approximate optimization (SAO) is recently used for improving the accuracy of the response surface [8-12]. In the SAO, the response surface is constructed repeatedly by adding new sampling points until terminal criteria are satisfied. In this paper, the SAO with the RBF network developed by the authors [17] is employed.

Here, we would like to summarize some issues to resolve as follows:

1. We focus on the BHG to avoid the defects in sheet forming. In the BHG approach in previous researches, an appropriate constant BHG is determined by trial-and-error method. In addition, the VBHG approach cannot be employed. In this paper, the VBHG approach is adopted.
2. Segmented blank holder shape can also play an important role to avoid the defects. In this paper, a segmented blank holder shape is also optimized. Therefore, the simultaneous optimization of both the VBGHs and the segmented blank holder shape is performed.
3. We investigate two comparative studies. Numerical results show that a better result can be obtained by the simultaneous optimization.

In this study, the risks of both wrinkling and tearing are evaluated by the Forming Limit Diagram (FLD). Both are then separately handled as the constraints in the optimization. An objective function is defined as the thickness deviation. The segmented blank holder shape and the VBHGs are taken as the design variables. Above optimization problem is solved by the SAO with the RBF network. LS-DYNA, which is one of the dynamic explicit Finite Element Analysis (FEA) codes, is employed in the numerical simulation.

The rest of this paper is organized as follows: In section 2, the FE-model and conditions are briefly described. The optimization problem of square cup deep drawing process will be formulated in section 3. Also, the SAO procedure with the RBF network will be briefly described. The optimization results by the SAO with the RBF network will be presented in section 4. Two comparative studies are also performed, and the advantage of the simultaneous optimization is discussed.

2. Finite Element Analysis Model

The FEA model taken from Ref. (6) is shown in Fig. 3. The material properties are listed in Table 1, which are obtained through the experiment. We have already examined the validity of the FEA model through an experiment with a constant BHF (100 [kN]) [6]. SPFC440 (Steel Plate Formability Cold) was selected as the test material. The blank size is 185[mm] x 185[mm], and the initial thickness is 1.20[mm]. In numerical simulation, 1/4 model is employed for the geometrical symmetry. Thus, a blank size of 92.5[mm] x 92.5[mm] is employed. The finite element models for the tools and the blank used in the square cup deep drawing are also shown in Fig. 3. The element type and the number of finite elements are tabulated in Table 2. A constant friction coefficient μ of 0.1 is used for all contact surfaces: blank/blank holder, blank/punch, blank/die, and blank/counter punch. A Belytschko-Tsay shell element with seven integration points across the thickness is used for

Table 1 Mechanical properties of blank sheet (SPFC 440)

Density: ρ [kg/mm^3]	7.84×10^{-6}
Young's modulus: E [MPa]	2.06×10^{5}
Poisson's ratio: ν	0.3
Yield stress: σ_Y [MPa]	353
Tensile strength: σ_T [MPa]	479
Normal anisotropy coefficient: r	0.98
Strain hardening coefficient: n	0.189

Table 2 Element type for numerical simulation

	Element type	Number of finite elements
Counter punch	Rigid	120
Dies	Rigid	924
Blank	Shell (Belytschko-Tsay)	2116
Blank holder	Rigid	432
Punch	Rigid	962

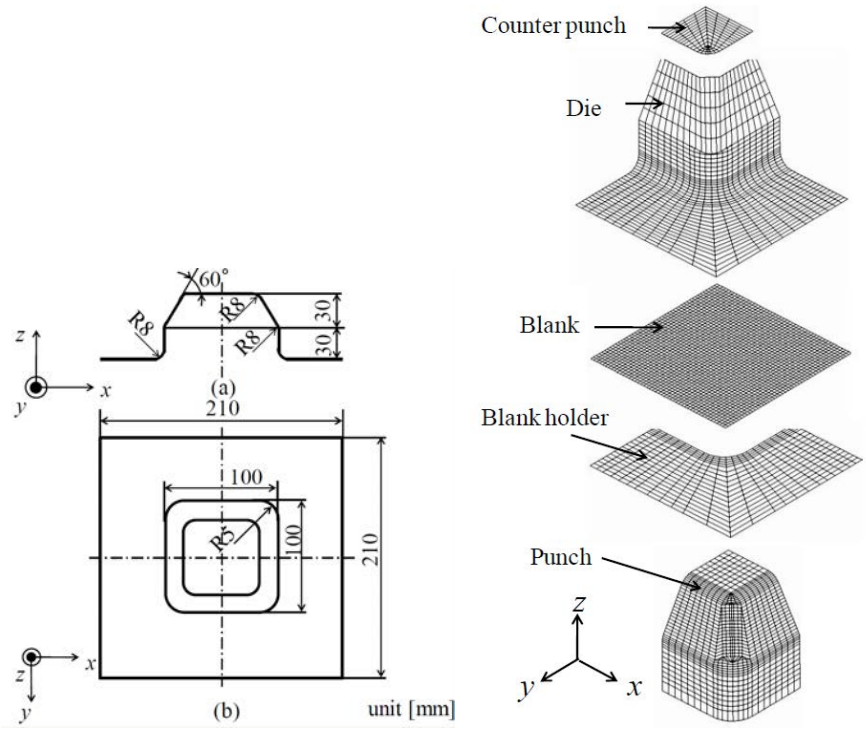

Fig. 3 Finite element model for square cup deep drawing process

the shell mesh of the blank. The relationship of stress-strain is approximately obtained from database in the LS- DYNA as follows:

$$\sigma = 793\varepsilon^{0.189} \tag{1}$$

3. Optimization Problem

3.1 Objective function

The maximum thickness leads to wrinkling, while the minimum thickness results in tearing. In sheet forming, it is preferable to minimize the thickness deviation. In this paper, the objective function is formulated as follow:

$$f(\boldsymbol{x}) = (t_{\max} - t_{\min})/t_0 \tag{2}$$

where $t_{\max}$ and $t_{\min}$ represent the maximum and minimum thickness of the blank after sheet forming, respectively. t_0 also represents the initial thickness of the blank before forming.

3.2 Design variables

The segmented blank holder shape and its BHGs are important factors to control the material flow. It is important to determine simultaneously them. Then, we consider them as the design variables. Here, let us explain how to take the design variables by using Fig. 4 (a)

and (b).

As shown in Fig. 4(a), the segmented blank holder shape A and D are taken as the design variables. The BHGs are applied to these segmented blank holder shape. In addition, the BHGs will vary through forming process for improving the product. Then, as shown in Fig. 4(b), the BHGs and its times are also taken as the design variables. As the result, the optimization problem in this paper consists of 8 design variables. Thus, $x_1(=BHG_{1,1})$, $x_2(=BHG_{1,2})$, $x_3(=BHG_{2,1})$, $x_4(=BHG_{2,2})$, $x_5(=T_1)$, $x_6(=T_2)$, $x_7(=A)$, and $x_8(=D)$. $BHG_{i,j}$ (i and j=1,2) represents the BHG of the i-th segmented blank holder shape at the j-th time period, T_j.

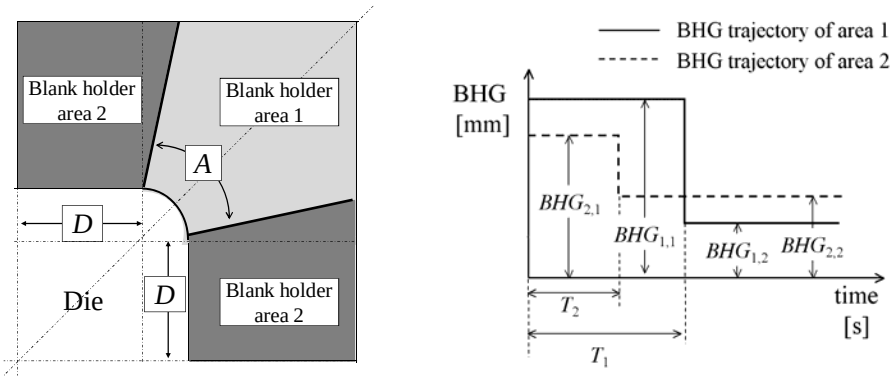

(a) Segmented blank holder shape (b) Variable BHGs

Fig. 4 Design variables

3.3 Constraints

As following a suggestion by Jakumeit et al. [18], it is natural to consider that the risk of both wrinkling and tearing can be handled as the constraints. According to their suggestion, we consider the defects as the constraints. In addition, wrinkling and tearing are handled separately as the constraints. In order to evaluate quantitatively the wrinkling and the tearing, the Forming Limit Diagram (FLD) is employed. In the FLD, strain states of all elements are plotted into major-minor strain plane. Let us consider the FLD as shown in Fig. 5.

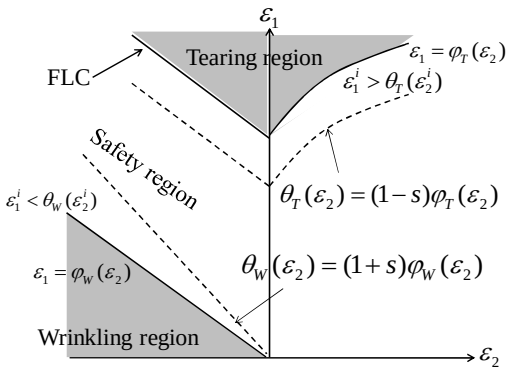

Fig. 5 Forming Limit Diagram (FLD)

In order to evaluate both wrinkling and tearing, the strains in the formed element are analyzed and compared against the Forming Limit Curve (FLC, as shown in Fig. 5).
We define the following FLC in the principal plane of logarithmic strains proposed by Hillman and Kubli [19].

$$\varepsilon_1 = \varphi_T(\varepsilon_2), \quad \varepsilon_1 = \varphi_W(\varepsilon_2) \tag{3}$$

where φ_T is one FLC which controls the tearing, and φ_W is also the other FLC which controls the wrinkling. Both of them depend on the material properties, which; they are

generally given as knots data in tables. Then, the following safety FLC is defined:

$$\theta_T(\varepsilon_2) = (1-s)\varphi_T(\varepsilon_2) \tag{4}$$

$$\theta_W(\varepsilon_2) = (1+s)\varphi_W(\varepsilon_2) \tag{5}$$

where s represents the safety tolerance, and is defined by the engineers. If some strain state of an element lies above the safety FLC θ_T, it is expected that a risk of tearing can be observed. Similarly, a risk of wrinkling can be assumed if the strain state of an element lies in the wrinkling region below the safety FLC θ_W. In numerical simulation, s is set to 0.2.

In order to clarify both risks, we examine separately the risk of both wrinkling and tearing. Referring to Ref. (20), the following two constraints are formulated:
For wrinkling:

$$g_1(x) = \begin{cases} \sum_{i=1}^{nelm} [\varepsilon_1^i - \theta_W(\varepsilon_2^i)] \exp[\varepsilon_1^i - \theta_W(\varepsilon_2^i)] & \varepsilon_1^i < \theta_W(\varepsilon_2^i) \\ 0 & \textit{Otherwise} \end{cases} \tag{6}$$

For tearing:

$$g_2(x) = \begin{cases} \sum_{i=1}^{nelm} [\varepsilon_1^i - \theta_T(\varepsilon_2^i)] \exp[\varepsilon_1^i - \theta_T(\varepsilon_2^i)] & \varepsilon_1^i < \theta_T(\varepsilon_2^i) \\ 0 & \textit{Otherwise} \end{cases} \tag{7}$$

where *nelm* denotes the total number of finite elements of the blank.

3.4 The procedure by the SAO with the RBF network

The procedure to find the optimum segmented blank holder shape and the VBHGs can be briefly summarized as follows:

(STEP1) Initial sampling points are generated.

(STEP2) Numerical simulation is carried out at the sampling points. The objective function and the constraints are evaluated.

(STEP3) Optimization is performed, and the optimal solution is added as the new sampling point.

(STEP4) The density function is optimized to find the unexplored region in the design variable space. The optimal solution of the density function is also added as the new sampling point.

(STEP5) When the terminal criterion is satisfied, the algorithm will be terminated. Otherwise, the algorithm will return to STEP2.

Various terminal criteria are considered. In this paper, we adopt the maximum number of sampling points as the terminal criterion. Therefore, the algorithm will be terminated at the maximum number of sampling points. The detailed procedure of the density function can be described in Ref. (17).

4. Numerical Results and Discussion

4.1 Numerical result by the proposed optimization problem

Optimization by the SAO with the RBF network is performed. 20 initial sampling points are generated by the Latin Hypercube Design (LHD). The maximum number of sampling points is employed as the terminal criterion of the SAO. In this numerical example, the maximum number of sampling points is set to 60. The side constraints of the design variables are also set as follows:

$$1.20 \le x_1, x_2, x_3, x_4 \le 2.25 \tag{8}$$

$$0.00 \le x_5, x_6 \le 0.81 \tag{9}$$

$$0.00 \le x_7 \le 90.00 \tag{10}$$

$$10.00 \le x_8 \le 45.00 \tag{11}$$

The optimum solution $\boldsymbol{x}_{opt} = (2.18, 1.41, 1.85, 1.36, 0.52, 0.16, 70.04, 17.02)^T$ could be obtained. The VBHGs trajectories and the segmented blank holder shape at $\boldsymbol{x}_{opt}$ are shown in Fig. 6(a) and (b).

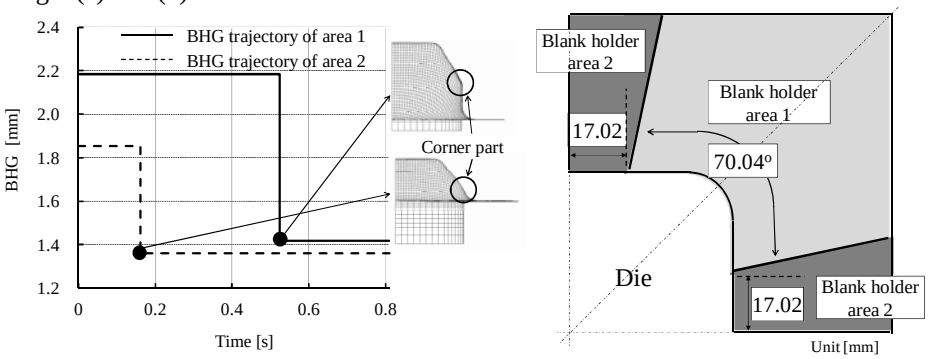

(a) VBHGs trajectories (b) Optimum segmented blank holder shape

Fig. 6 Results at the optimum point

In practical sheet forming, the tearing can be often observed at a corner part of products. In order to avoid the tearing, larger BHGs are applied before forming of the corner part for the activation of material flow into the die. After that, the BHGs are decreasing. Figure 6(a) roughly corresponds to the practical sheet forming.

In sheet forming, the tearing should be strongly avoided in comparison with wrinkling. Then, the following two detection criteria for the tearing are employed: One is to use the FLD, and the other is the minimum thickness. When the minimum thickness is employed for the tearing detection criterion, a critical value is determined in advance. If the minimum thickness is smaller than the critical value, we suppose that the tearing can be observed. According to our previous works [6, 12], the critical value of the thickness is set to 0.9[mm] ($=t_0$ x 0.75). Figure 7 (a) and (b) shows the FLD and the thickness distribution. It can be found from Fig. 7(a) that no elements can be observed in the tearing region. In addition, the minimum thickness is larger than 0.9 [mm]. It is clear from these results that no tearing can be observed.

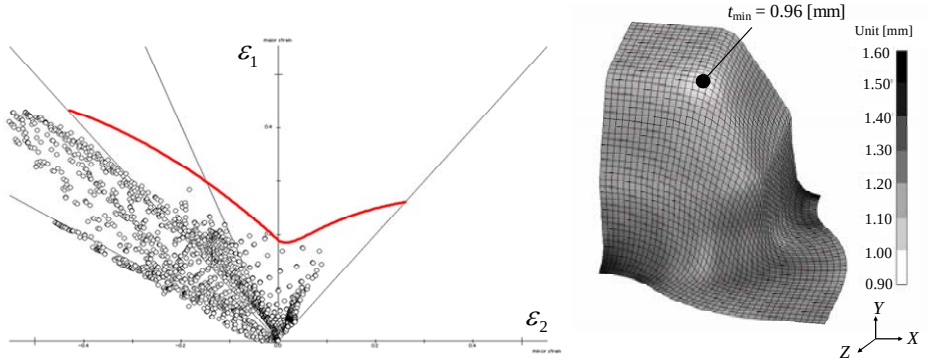

(a) FLD at the optimum solution (b) Thickness distribution

Fig. 7 FLD and thickness distribution at the optimum point

4.2 Comparative studies

In order to examine the validity of the proposed approach, the following two cases are examined:

Case I: The segmented blank holder shape is fixed. The BHGs ($BHG_1 = x_1$ and $BHG_2 = x_2$) shown in Fig. 8 are taken as the design variables, and the BHGs are fixed through forming process. Therefore, the number of design variables is 2. The lower and upper bounds of the design variables are given as follows:

$$1.20 \le x_1, x_2 \le 2.25 \tag{12}$$

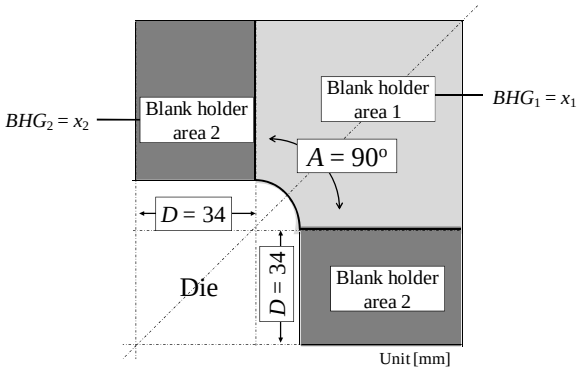

Fig. 8 Design variables in Case I

Case II: In addition to the design variables of case I, the angle $A(=x_3)$ and the distance $D(=x_4)$ in Fig. 8 are also taken as the design variables. The BHGs also fixed through forming process. Therefore, the number of design variables is 4. The lower and upper bounds of x_3 and x_4 are given as follows:

$$0.00 \le x_3 \le 90.00 \tag{13}$$

$$10.00 \le x_4 \le 45.00 \tag{14}$$

The optimum point of case I is found as $\boldsymbol{x}_{opt}^{\mathrm{I}} = (1.53, 1.21)^T$. Figure 9(a) and (b) shows the FLD and the thickness distribution with the minimum thickness. It can be found from Fig. 9(a) and (b) that no tearing can be observed.

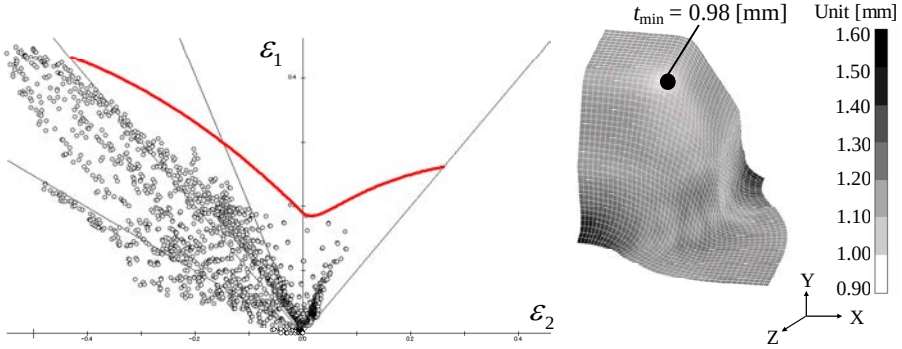

(a) FLD of case I (b) Thickness distribution of case I

Fig. 9 Results of Case I

Next, the optimum point of case II is obtained as $\boldsymbol{x}_{opt}^{\mathrm{II}} = (2.21, 1.23, 89.38, 12.53)^T$. The segmented blank holder shape at $\boldsymbol{x}_{opt}^{\mathrm{II}}$ is shown in Fig. 10. Similar to case I, the FLD and the thickness distribution with the minimum thickness are shown in Fig. 11(a) and (b).

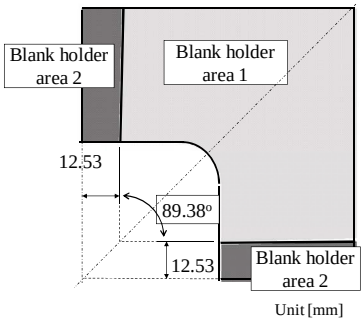

Fig. 10 Optimum segmented blank holder shape of case II

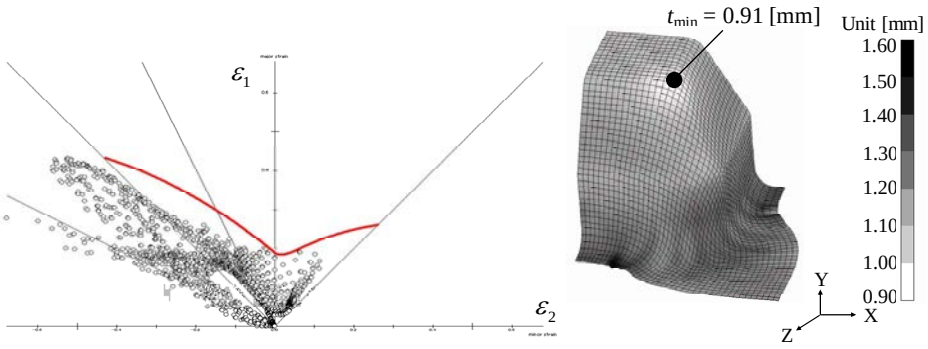

(a) FLD of case II (b) Thickness distribution of case II

Fig. 11 Results of Case II

4.3 Discussions

Above all results could be obtained by the response surface with the RBF network. First the accuracy of the response surfaces in all cases is examined. All functions (objective and two constraints) are separately approximated. Figures 12 through 14 show the accuracy of all functions. It can be found from Fig. 12 that highly accurate response surfaces have been obtained.

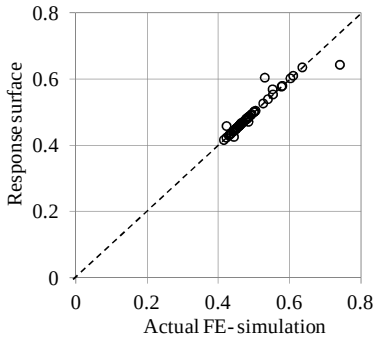

(a) Accuracy of the objective function

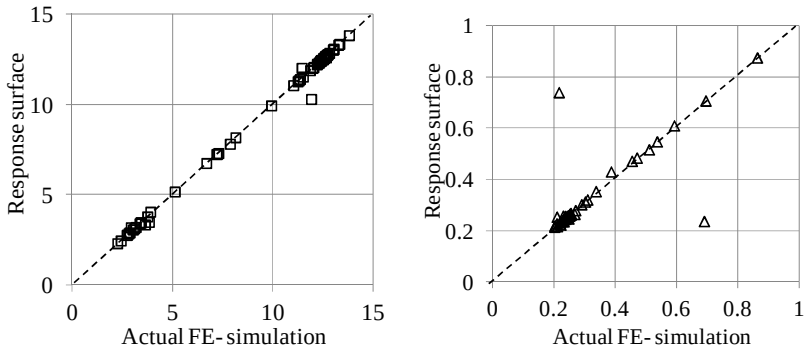

(b) Accuracy of the constraint (Wrinkling) (c) Accuracy of the constraint (Tearing)

Fig. 12 Accuracy of the response surfaces in the proposed approach

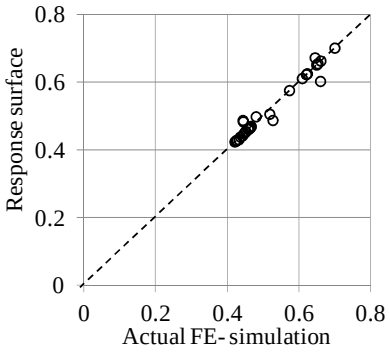

(a) Accuracy of the objective function

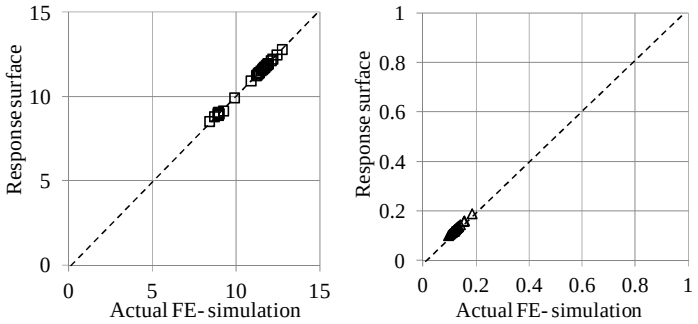

(b) Accuracy of the constraint (Wrinkling) (c) Accuracy of the constraint (Tearing)

Fig. 13 Accuracy of the response surfaces in case I

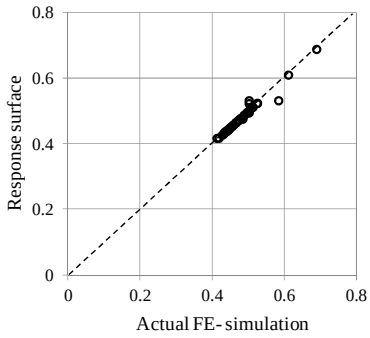

(a) Accuracy of the objective function

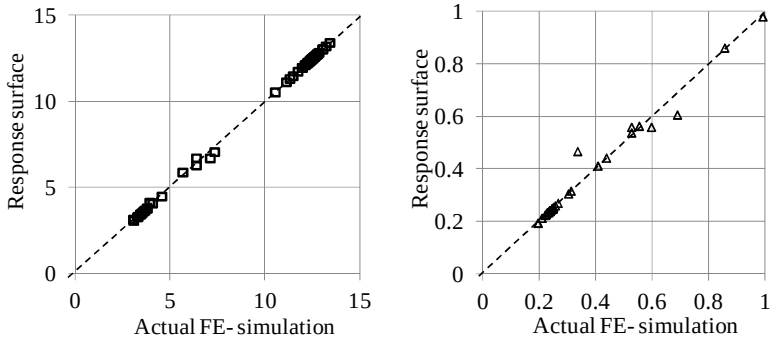

(b) Accuracy of the constraint (Wrinkling) (c) Accuracy of the constraint (Tearing)

Fig. 14 Accuracy of the response surfaces in case II

Each objective at the optimum is listed in Table 3. It can be found that the objective by the proposed approach is better than others.

Table 3 Comparison of each objective at the optimum

	Propose approach	Case I	Case II
Objective	0.485	0.519	0.502

Finally, results of all cases are discussed. As already described in section 4.1, the tearing should be strongly avoided in the sheet forming process. We then discuss results of all cases on the tearing and the objective function. It can be found from the FLD and the thickness distribution of all cases that no tearing can be observed. Note that two tearing detection criteria are employed in this paper. One is based on the FLD, and the other is the minimum thickness.

In case I, two BHGs are optimized under the fixed segmented blank holder shape, which are not varied through the punch stroke. Though no tearing can be observed, the objective at the optimum is worst among three cases.

In case II, the segmented blank holder shape and its BHGs are optimized. Similar to case I, the BHGs do not vary through the punch stroke. The objective at the optimum is improved in comparison with case I. This result implies that the segmented blank holder shape plays an important role for improving the product.

Finally, in the proposed approach, the segmented blank holder shape and its VBHGs are optimized simultaneously. It is clear from Table 3 that the best objective can be obtained. In the proposed approach, the VBHG trajectories are also obtained. We can find from case II that the segmented blank holder shape plays an important factor for improving the product. In addition, the VBHGs trajectories also are important factor.

5. Concluding Remarks

In this paper, variable blank holder gap (VBHG) trajectory and segmented blank holder shape were optimized simultaneously. In the past researches, a blank holder gap for avoiding the wrinkling and the tearing was manually determined, and a constant gap was employed. Finding the VBHG trajectory is one of the challenging themes in sheet forming. In addition, the optimum segmented blank holder shape is also considered. A sheet forming simulation is generally a time consuming task, and then the sequential approximate optimization with radial basis function network is employed. The forming limit diagram is used to detect quantitatively the wrinkling and the tearing. The thickness deviation is taken as the objective function. In order to compare the result by the proposed approach, two comparative studies were examined. By comparing with two results of the comparative studies, the result by the proposed approach showed better result. In particular, the simultaneous optimization of both the segmented blank holder shape and the gaps will lead to the improvement of product quality.

References

(1) Metal Forming Handbook /Schuler Springer-Verlag, (1998), Berlin Heidelberg.

(2) Sheng, Z.Q., Jirathearanat, S., and Altan, T., Adaptive FEM Simulation for Prediction of Variable Blank Holder Force in Conical Cup Drawing, *International Journal of Machine Tools and Manufacture*, Vol. 44, No. 5, (2004), pp. 487-494.

(3) Lin, Z.Q., Wang, W.R., Chen, G.L., A New Strategy to Optimize Variable Blank Holder Force towards Improving the Forming Limit of Aluminum Sheet Metal Forming. *Journal of Materials Processing Technology*, Vol. 183, No. 2-3, (2007), pp. 339-346.

(4) Wang, W.R., Chen, G.L., Lin, Z.Q., and Li, S.H., Determination of Optimal Blank Holder Force Trajectories for Segmented Binders of Step Rectangle Box using PID Closed-loop FEM Simulation, *International Journal of Advanced Manufacturing Technology*, Vol. 32, No. 11, (2007), pp. 1074-1082.

(5) Lo, S.W., and Yang, T.C. Closed-loop control of the blank holding force in sheet metal forming with a new embedded-type displacement sensor, *International Journal of Advanced Manufacturing Technology*, Vol. 24, (2004), pp.553-559.
(6) Kitayama, S., Hamano, S., Yamazaki, K., Kubo, T., Nishikawa H, and Kinoshita H., A Closed-loop Type Algorithm for Determination of Variable Blank Holder Force Trajectory and its Application to Square Cup Deep Drawing, *International Journal of Advanced Manufacturing Technology*, Vol. 51, No. 5, (2010), pp. 507-517.
(7) Chengzhi, S., Guanlong, C., and Zhongqin, L., Determining the optimum variable blank-holder forces using adaptive response surface methodology (ARSM), *International Journal of Advanced Manufacturing Technology*, Vol. 26, No.1, (2005), pp. 23-29.
(8) Wang, H., Li, G.Y., and Zhong, Z.H., Optimization of Sheet Metal Forming Processes by Adaptive Response Surface Based on Intelligent Sampling Method, *Journal of Materials Processing Technology*, Vol.197, No. 1-3, (2008), pp. 77-88.
(9) Wang, H., Enying, L., and, Li, G.Y., Parallel Boundary and Best Neighbor Searching Sampling Algorithm for Drawbead Design Optimization in Sheet Metal Forming, *Structural and Multidisciplinary Optimization*, Vol.41, No. 2, (2010), pp. 309-324.
(10) Wang, H., Enying, L., and, Li, G.Y., Optimization of Drawbead Design in Sheet Metal Forming Based on Intelligent Sampling by Using Response Surface Methodology, *Journal of Materials Processing Technology*, Vol. 206, No. 1-3, (2008), pp. 45-55.
(11) Wang, H., Enying, L., and Li, G.Y., Zhong, ZH., Optimization of Sheet Metal Forming Processes by the Use of Space Mapping Based Metamodeling Method, *International Journal of Advanced Manufacturing Technology*, Vol. 39, No. 7, (2008), pp. 642-655.
(12) Kitayama, S., Kita, K., and Yamazaki, K., Optimization of Variable Blank Holder Force Trajectory by Sequential Approximate Optimization with RBF network, *Journal of Advanced Manufacturing Technology*, DOI 10.1007/s00170-011-3755-y, (Online available).
(13) Osakada, K., Mori, K., Atlan, T., and Groche, P., Mechanical Servo Press Technology For Metal forming, *CIRP Annals - Manufacturing Technology*, Vol. 60, No. 2, (2011), pp. 651-672.
(14) Wang, H., Xu, W., Lin, Z.Q., Yang, Y., and Wang, Z.R., Stamping and Stamping Simulation with Blankholder Gap, *Journal of Materials Processing Technology*, Vol. 120, No. 1-3, (2002), pp. 62-67.
(15) Chen, L., Yang, J.C., Zhang, L.W., and Yuan, S.Y., Finite Element Simulation and Model Optimization of Blank Holder Gap and Shell Type in the Stamping of Washing-trough, *Journal of Materials Processing Technology*, Vol. 182, No. 1-3, (2007), pp. 637-643.
(16) Gavas, M., and Izciler, M., Effect of Blank Holder Gap on Deep Drawing of Square Cups, *Materials and Design*, Vol. 28, No. 5, (2008), pp. 1641-1646.
(17) Kitayama, S., Arakawa, M., and Yamazaki, K., Sequential Approximate Optimization using Radial Basis Function network for engineering optimization, *Optimization and Engineering*, Vol. 12, No. 4, (2010), pp. 535-557.
(18) Jakumeit, J., Herdy, M., and Nitsche, M., Parameter Optimization of the Sheet Metal Forming Process Using an Iterative Parallel Kriging Algorithm, *Structural and Multidisciplinary Optimization*, Vol. 29, (2005), pp. 498-507.
(19) Hillmann, M., and Kubli, W., Optimization of Sheet Metal Forming Processes Using Simulation Programs, *In: Numisheet 99*, Vol.1, (1999), pp. 287-292.
(20) Guangyong, S., Guangyao, L., Shiwei, Z., Wei, X., Xuying, Y., and Qing, L., Multi-fidelity Optimization for Sheet Metal Forming Process, *Structural and Multidisciplinary Optimization*, Vol. 44, No. 1, (2011), pp. 111-124.